JOURNAL OF MATERIALS SCIENCE 33 (1998) 189–197

Determining the toughness of plastically deforming joints

M. D. THOULESS, J. L. ADAMS, M. S. KAFKALIDIS
Department of Mechanical Engineering & Applied Mechanics, University of Michigan, Ann Arbor, MI48109-2125, USA

S. M. WARD, R. A. DICKIE, G. L. WESTERBEEK
Ford Research Laboratory, Ford Motor Company, Dearborn, MI48121-2053, USA

An analysis is presented for the fracture of an adhesively bonded double-cantilever beam that fails with extensive plastic deformation of the adherends. The analysis permits a value for the toughness of the joint to be distinguished from the energy absorbed by the plastic deformation. Specifically, this value for toughness can be determined from post-fracture observations of the deformation and from a knowledge of the constitutive properties of the adherends. The analysis has been used to determine experimentally the toughness of plastically deforming joints formed using three different adhesives to bond a series of different thicknesses of aluminium and steel. In each case, it was found that, despite large differences in the extent of deformation, the value for toughness was dependent only on the materials used to form the joint. The toughness was independent of the thickness of the adherends.

1. Introduction

The use of adhesives to replace traditional joining techniques has many advantages for the automative industry. A major advantage is related to the current trend towards energy efficiency and the consequent need to reduce the weight of vehicles. Spot-welding, which is the traditional fabrication technique for steel structures, is difficult in light-weight substitute materials, such as aluminium, and impossible with some modern materials of interest, such as composites and polymers. These materials can be joined with adhesives. Furthermore, it has been shown that an adhesively-bonded structure can exhibit up to 45% greater stiffness than an equivalent spot-welded structure, with no increase in mass [1]. In addition to these weight-saving issues, there are other advantages of adhesives. Empirical evidence indicates that the fatigue life of an adhesive joint can be much greater than that of spot-welded joints. There is also an aesthetic advantage to the use of adhesives because body sheet metal can be assembled with smooth surfaces; the need for additional trim to hide spot welds is therefore eliminated.

While engineers have collectively accumulated a vast body of experience with incorporating traditional joining techniques into the design process, the same is not true for adhesives. Therefore, despite the many advantages of adhesives, a number of fundamental issues need to be addressed before it is possible to use adhesives confidently in structurally critical components. The most important is how to predict the reliability of a joint under service conditions, and, of particular importance for automotive applications, is how an adhesively bonded structure will absorb energy during impact loading.

There is a considerable body of literature dealing with stress analyses of adhesive joints and ASTM-approved test techniques [2]. Unfortunately, the data that can be obtained from many of these tests do not have a predictive capability; they merely provide a means of process control and a qualitative comparison of adhesives under particular test conditions. However, it is being increasingly recognized that the failure of adhesive joints is governed by the principles of fracture mechanics. Provided measurements are made using specimens of a suitable geometry, i.e. containing well-defined cracks and with sufficiently thick adherends to ensure only elastic deformation, the concepts of linear-elastic fracture mechanics (LEFM) should apply. Using these concepts, it has been shown experimentally that the mechanical properties of symmetrical adhesive joints are described in a predictive fashion by the use of a toughness or a "mode-I critical energy-release rate", $\mathcal{G}_{Ic}$ [3, 4].

Designing a car for crash-worthiness involves ensuring that during impact, carefully chosen structural members will deform plastically and absorb energy. Therefore, the design criteria for using structural adhesives in automotive applications need to be determined under impact conditions with extensive plastic deformation occurring. Under these conditions, LEFM techniques are not applicable because most of the energy dissipated does not go into fracturing the adhesive, but rather into other processes that are

0022–2461

specimen specific, such as friction and plastic deformation of the substrate. Analyses of the peel test by Kim and others [5, 6] illustrate the inherent problems in determining the properties of an adhesive joint under such conditions, because the toughness of the adhesive accounts for only a small fraction of the total energy dissipated during fracture.

How to develop a framework for analysing crack growth in the presence of extensive non-linear deformation is a problem that has been considered for many years [7–10]. One inherent philosophical difficulty is how to distinguish the energy associated with the crack-tip plastic zone from that associated with macroscopic plastic deformation. If this cannot be done, the concept of toughness as a material or interfacial property loses its usefulness, because the conditions under which a crack will propagate cannot be predicted; they would have to be determined experimentally for each and every configuration of interest. In the present case of a confined adhesive, a simple separation of the energy dissipation into that associated with the adhesive and that associated with the substrates can be rationalized [9]. The energy dissipated within the adhesive, per unit area of crack advance, can then be designated as the "toughness" of the joint. Such an analysis is provided in this paper, and the results are used to evaluate the toughness of different configurations of joints loaded by a wedge under impact conditions.

2. Analysis

The general problem considered in this paper is illustrated in Fig. 1. It consists of an adhesively bonded double-cantilever beam with arms 1 and 2 of thickness h_1 and h_2, respectively, with an equal moment, M_o applied to each arm. If the adherends are elastic, then the crack-driving force, or energy-release rate, $\mathcal{G}$, is given by [11]

$$\mathcal{G} = \frac{6M_0^2}{Eb^2}\left(\frac{1}{h_1^3} + \frac{1}{h_2^3}\right) \tag{1}$$

in plane stress, where E is Young's modulus of the adherends, and b is the width of the specimen. This expression is invalid if the magnitude of the moment required to propagate the crack is sufficiently large that the arms deform plastically. Generally, caution has to be used in deriving expressions for crack-driving forces in the presence of plasticity because they will be invalidated by any hysteresis associated with unloading [7]. However, in the special case of the problem illustrated in Fig. 1, an analysis based on the steady-state geometry permits a rigorous expression for the crack-driving force to be derived.

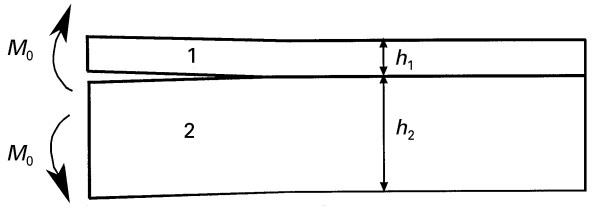

Figure 1 The asymmetrical double-cantilever specimen considered in this analysis. Two pieces of material of thickness h_1 and h_2, respectively, are bonded across an interface. A moment M_o is applied to each arm.

It is assumed that both arms are made of materials that exhibit a stress–strain relationship of the following form

$$\sigma = A_i\varepsilon^{n_i} \tag{2}$$

where σ and ε are the stress and strain, n_i is the power-law hardening exponent, A_i is a material constant, and the subscript i identifies the arm, 1 or 2. Furthermore, it is assumed that all strains remain small so that simple beam theory can be used, and that the crack is long enough for steady-state conditions to apply. Consider what happens if a length δl ahead of the crack tip debonds under the influence of the bending moment M_o. Owing to the steady-state nature of the problem, the changes in energy and work associated with this debonding can be analysed by considering what would happen if a segment of the same length, δl is removed from the region far ahead of the crack and placed in its wake. Ahead of the crack, both parts of the segment above and below the interface are undeformed. When placed in the wake, they are bent into arcs of circles by the moments, M_o. Using simple beam theory, it can readily be shown that the resultant radii of curvature are given by

$$R_i = \left[\frac{bA_ih_i^{n_i+2}}{2^{n_i+1}(n_i+2)M_o}\right]^{1/n_i} \tag{3}$$

The energy stored in each arm of the segment is

$$U_i = \int_0^{\theta_j} M d\theta = \frac{bA_ih_i^{n_i+2}}{2^{n_i+1}(n_i+2)(n_i+1)R_i^{n_i+1}}\,\delta l \tag{4}$$

where $\theta = \delta l/R$. Furthermore, the work done on each arm by the applied moment is

$$W_i = M_o\theta_i = M_o\delta l/R_i = \frac{bA_ih_i^{n_i+2}}{2^{n_i+1}(n_i+2)R_i^{n_i+1}}\,\delta l \tag{5}$$

where R_i is given by Equation 3. The driving force for crack growth is then given by

$$\mathcal{G} = \frac{(W_1+W_2)-(U_1+U_2)}{b\delta l} \tag{6}$$

Therefore, from Equations 4 and 5

$$\mathcal{G} = \sum_{i=1,2}\frac{A_in_i}{2^{n_i+1}(n_i+2)(n_i+1)}\frac{h_i^{n_i+2}}{R_i^{n_i+1}} \tag{7}$$

This expression can be re-expressed in terms of M_o by the use of Equation 3. For example, if both arms are made of the same material then

$$\mathcal{G} = \frac{2M_on}{b(n+1)}\left[\frac{2(n+2)M_o}{Ab}\right]^{1/n}\left(\frac{1}{h_1^{1+(2/n)}} + \frac{1}{h_2^{1+(2/n)}}\right) \tag{8}$$

which, in the linear case of $n = 1$ reduces to Equation 1. In this steady-state case where there is no change in the loading in the wake of the crack, this solution can also be obtained directly using the definition of an energy-release rate, $\mathcal{G} = \partial(W - U)/b\partial a$, where W is the work done by the applied moments, U is the strain energy in the system, and a is the crack length [10].

The energy-release rate increases with the bending moment until its magnitude reaches the toughness, Γ. At this point, the crack propagates. Provided the constitutive properties of the adherends are known, the toughness of the joint can be measured by determining the bending moment, M_p, required to cause debonding. For example, in the symmetrical case when $h_1 = h_2 = h$, the toughness is given by

$$\Gamma = \frac{4M_{\mathrm{p}}n}{b(n+1)}\left[\frac{2(n+2)M_{\mathrm{p}}}{Abh^{n+2}}\right]^{1/n} \tag{9}$$

An equivalent expression can be readily obtained from Equations 3 and 7 for the general case where the arms are of different thicknesses and made of different materials.

It is also possible to deduce Γ without directly measuring M_{p}. Provided the toughness does not vary along the interface, the substrates will deform into a constant radius of curvature, R_{p}, along the debonded portion. R_{p} is related to M_{p} by Equation (3) so that, in terms of R_{p}, the toughness of the adhesive is given by

$$\Gamma = \frac{Anh^{n+2}}{2^n(n+2)(n+1)R_{\mathrm{p}}^{n+1}} \tag{10}$$

Consequently, the toughness can be determined by measuring the radius of curvature of the fractured specimens, and from a knowledge of the constitutive properties of the adherend. This is the procedure followed in the experiments described below.

3. Experimental procedure

A series of symmetrical test specimens (Fig. 2) was prepared from coupons cut from different thicknesses of sheets of pretreated and prelubricated aluminium (5754 aluminium, Alcan Rolled Products Co.) and cold-rolled steel (draw-quality, special-killed, cold-rolled steel, Inland Steel Co. with a nominal yield stress of 170–240 MPa). The thicknesses of the aluminium samples were 1.0, 1.3, 1.6, 2.0, 2.6 and 3.0 mm; the thicknesses of the steel samples were 0.5, 0.7, 0.9, 1.1 and 1.4 mm. The specimens were 90.0 mm long and 20.0 mm wide. They were bonded with one of three commercial toughened epoxies [described as adhesives A (Ciba-Geigy LMD 1142), B (Ciba-Geigy XD4600) and C (Essex 73 301)] and cured at 180 °C for 30 min in an air-circulating oven. The bond length was 30.0 mm and was established by placing a strip of Teflon tape, 12.7 mm wide, across each coupon 30 mm from the ends of the coupon. The thickness of the bondline was controlled by sprinkling a few glass beads of diameter 0.25 mm on the adhesive, and then clamping the coupons together during curing. After curing, the sides and ends of the sample were cleaned and excess adhesive was removed by filing.

Impact fracture tests were performed at room temperature (21 °C) on an instrumented impact test machine (Dynatup, General Research Corp., Model GRC 8250) employing a drop weight [12]. The test samples were placed over a hardened steel wedge with a tip radius of 1.0 mm, and a wedge angle of 10°. The tip of the wedge was aligned with a locating mark scribed on the side of the sample, 10.0 mm from the edge of the adhesive. The impact of the weight forced the wedge through the specimen, causing the arms of the specimen to bend and the adhesive to fracture (Fig. 3). The initial height of the hammer, which had a mass of 44.85 kg was set so that the velocity upon striking the sample was $2 \pm 0.2\ \mathrm{m\,s^{-1}}$. An accelerometer located in the hammer was used to measure the deceleration as a function of time, so that the velocity of the hammer, the load applied to the sample and the energy dissipated during the test could be calculated.

An example of the deformation of the fractured samples can be seen in the photograph of Fig. 4. In particular, the approximately constant radius of curvature in the region of the adhesive that resulted during fracture should be noted. This suggests that fracture occurred under conditions of a constant moment, and the analysis of the previous section can be used to determine the toughness of the joint. The radii were calculated from the rectangle properties of chords using measurements made by a ruler on the magnified shadow of the test specimens projected on a screen. It was noted that the adherends on either side

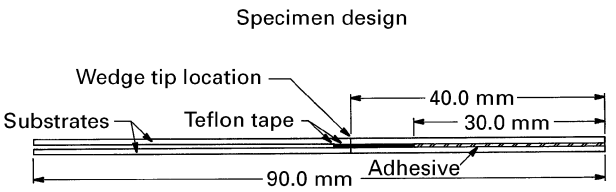

Figure 2 The test configuration consisted of two 90 mm length metal coupons of equal thickness bonded over the last 30 mm of their lengths.

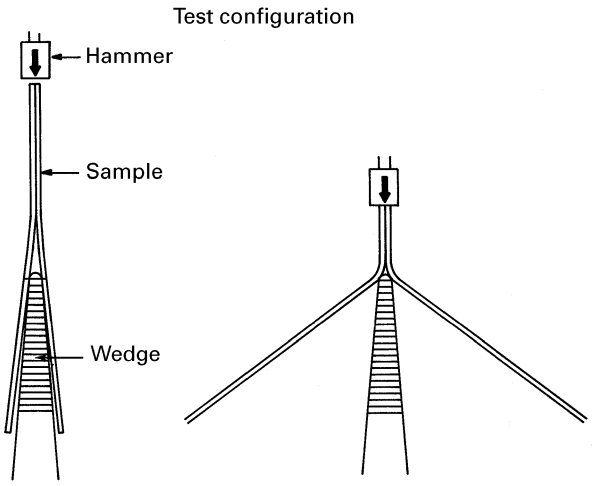

Figure 3 The experimental configuration during the tests in which the test samples were split by being driven over a wedge under the impact of a hammer.

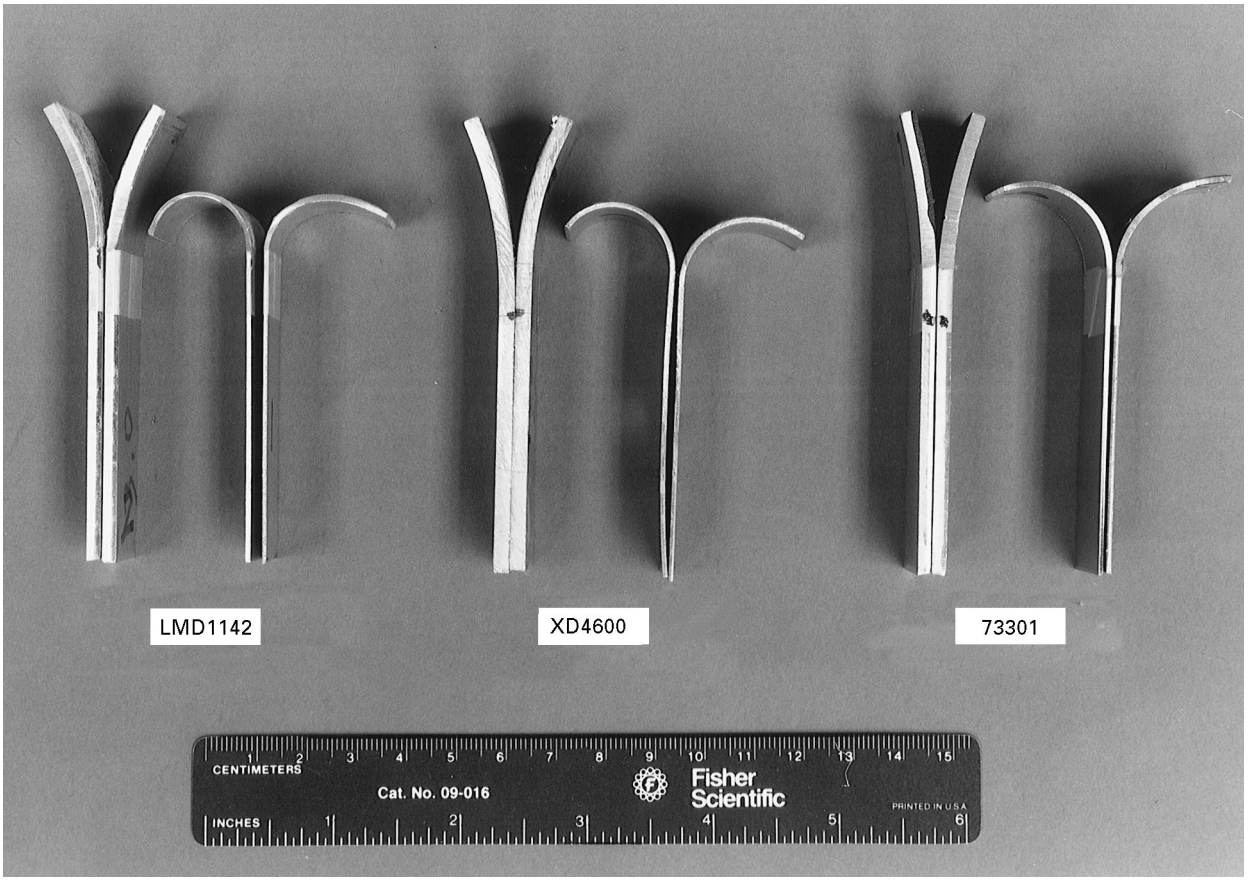

Figure 4 Photograph of a failed test specimen, showing the curvature in the region where debonding occurred.

of the bond generally deformed to different amounts, giving two radii of curvature, R_1 and R_2. This suggests that the sample was not always placed perfectly symmetrically on the wedge so, when the hammer struck it, the sample rotated slightly. A weighted mean of R_1 and R_2 was therefore defined from Equation 7 as

$$R_p = \left(\frac{2}{R_1^{n+1} + R_2^{n+1}}\right)^{1/(n+1)} R_1 R_2 \qquad (11)$$

and used in Equation 10 to obtain the toughness of the joint. This definition of R_p is identical to using R_1 and R_2 to compute the contributions to the energy-release rate of both arms separately, and then adding them. It can be shown that the imbalance in moments this difference in radii implies has an insignificant effect on the toughness values obtained. The additional bending moment required for equilibrium has therefore been ignored. Furthermore, the effects of elastic spring-back were also ignored because calculations determined that they did not significantly affect the results in the present case. Therefore, the measured curvatures were used without modification to give R_p.

In a second phase of experimentation, dogbone tensile coupons, approximately 12×150 mm were cut from each thickness of the metal sheets and fitted with a 50 mm clip gauge. These coupons were tested to failure in uniaxial tension using a mechanical testing machine. The resultant stress–strain data were fitted to a power-law relationship. Particular attention was paid to fitting the data over the range 0–10%, because this was the appropriate range of deformation for the fractured samples. An example of the data and such a fit is shown in Fig. 5. The resulting power-law expression was used in Equation 10, with the measured results for the plastic radius of curvature, to deduce values for the toughness of the adhesive. The experimental results are tabulated fully in Table I (for the aluminium samples) and in Table II (for the steel samples).

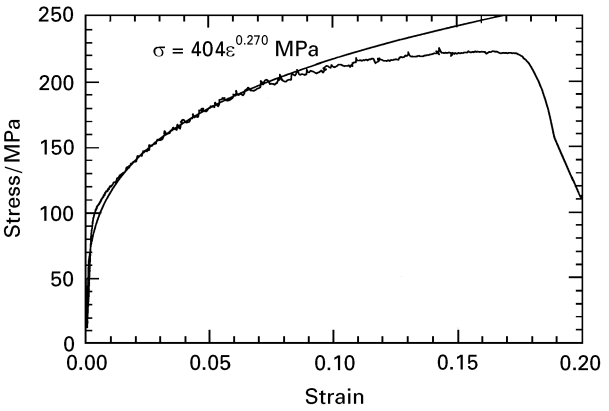

Figure 5 Tensile stress–strain curve for a 1.6 mm thick aluminium sheet with the power-law fit used to analyse the data ($A = 404$ MPa, $n = 0.270$).

The calculations allow the total energy absorbed during fracture to be partitioned between the work done to fracture the adhesive, the work done deforming the metal, and the energy dissipated in other

TABLE I Results for aluminium bonded with adhesives A (LMD1142), B (XD4600) and C (Essex 73301)

Thickness (mm)	A (MPa)	n	R_1, R_2 (mm)	R_p (mm)	Γ (kJ m^{-2})
Adhesive A					
1.01	424	0.271	9, 12	10	1.69 ± 0.25
			9, 14	11	
			15, 8	10	
			9, 13	11	
			8, 16	10	
1.31	366	0.234	12, 18	14	1.92 ± 0.30
			11, 17	13	
			11, 17	13	
			12, 18	14	
			11, 18	14	
1.61	404	0.270	18, 21	19	2.13 ± 0.32
			18, 24	20	
			17, 24	20	
			23, 16	19	
			16, 23	19	
2.00	346	0.227	29, 26	27	1.97 ± 0.30
			27, 27	27	
			24, 30	26	
			25, 32	28	
			27, 30	28	
2.30	355	0.235	38, 32	35	2.04 ± 0.31
			39, 36	38	
			31, 34	32	
			41, 34	37	
			37, 32	34	
3.00	367	0.238	67, 54	60	1.94 ± 0.29
			57, 60	58	
			57, 60	58	
			57, 63	60	
			67, 71	70	
Adhesive B					
1.01	424	0.271	10, 20	13	1.33 ± 0.20
			10, 16	12	
			10, 19	13	
			10, 24	14	
			11, 14	12	
1.31	366	0.234	15, 24	19	1.30 ± 0.21
			17, 20	19	
			15, 30	19	
			15, 23	18	
			15, 26	19	
1.61	404	0.270	20, 31	24	1.56 ± 0.23
			22, 32	25	
			21, 34	26	
			20, 34	25	
			20, 30	24	
2.00	346	0.227	30, 45	36	1.36 ± 0.21
			33, 44	37	
			31, 45	36	
			34, 40	37	
			35, 45	39	
2.30	355	0.235	39, 47	42	1.56 ± 0.25
			42, 55	47	
			42, 54	47	
			38, 47	42	
			39, 41	40	
3.00	367	0.238	78, 90	84	1.43 ± 0.21
			74, 79	76	
			64, 92	75	
			65, 83	73	
			77, 82	80	

TABLE I (Continued).

Thickness (mm)	A (MPa)	n	R_1, R_2 (mm)		R_p (mm)		Γ (kJ m^{-2})
Adhesive C							
1.01	424	0.271	20, 16	18, 18	18	18	0.83 ± 0.12
			15, 28	26, 16	19	19	
			24, 15	16, 21	19	18	
			15, 24	16, 22	18	18	
			16, 22	19, 18	18	18	
1.31	366	0.234	23, 32	22, 40	27	28	0.80 ± 0.12
			24, 31	24, 31	27	27	
			24, 38	23, 36	29	28	
			24, 26	24, 39	25	30	
			23, 41	33, 24	29	28	
1.61	404	0.270	49, 31	46, 32	37	37	0.96 ± 0.14
			31, 48	47, 30	37	37	
			30, 47	48, 31	36	37	
			31, 46	39, 33	37	35	
			41, 30	31, 47	35	37	
2.00	346	0.227	48, 64	46, 67	55	54	0.89 ± 0.13
			44, 63	45, 65	52	53	
			76, 45	46, 69	56	55	
			44, 62	44, 55	51	48	
			45, 60	43, 70	51	53	
2.30	355	0.235	57, 77	55, 84	66	66	0.92 ± 0.17
			90, 56	76, 57	69	65	
			58, 71	86, 57	64	69	
			52, 76	59, 78	62	67	
			86, 55	60, 84	67	70	
3.00	367	0.238	131, 101	102, 128	114	113	0.92 ± 0.20
			102, 92	98, 113	97	105	
			125, 114	98, 160	119	121	
			112, 87	98, 149	98	118	
			128, 115	115, 93	121	103	

TABLE II Results for steel bonded with adhesives A (LMD1142), B (XD4600) and C (Essex 73301)

Thickness (mm)	A (MPa)	n	R_1, R_2 (mm)		R_p (mm)		Γ (kJ m^{-2})
Adhesive A							
0.52	433	0.094	None of the samples fractured		?		?
0.71	422	0.152	Most of the samples did not fracture		?		?
0.91	440	0.158	11, 14	10, 15	12	12	1.14 ± 0.17
			13, 14	10, 15	14	12	
			10, 15	11, 13	12	12	
			10, 14	11, 14	12	12	
			10, 14	9, 16	12	12	
1.14	398	0.131	13, 22	17, 13	16	15	1.14 ± 0.17
			17, 16	13, 17	16	15	
			13, 17	17, 16	15	17	
			16, 18	15, 19	17	17	
			13, 20	15, 17	16	16	
1.41	439	0.124	23, 21	26, 19	22	22	1.33 ± 0.20
			27, 18	19, 24	21	21	
			19, 27	27, 21	22	24	
			28, 18	18, 30	22	22	
			18, 27	27, 24	22	25	

TABLE II (Continued).

Thickness (mm)	A (MPa)	n	R_1, R_2 (mm)		R_p (mm)		Γ (kJ m^{-2})
Adhesive B							
0.52	433	0.094	Only some of the samples fractured		?		?
0.71	422	0.152	11, 10	15, 10	10	12	0.71 ± 0.11
			15, 10	12, 11	12	11	
			12, 10	12, 9	11	11	
			13, 10	12, 10	11	11	
			13, 10	10, 9	11	10	
0.91	440	0.158	17, 15	17, 14	16	16	0.86 ± 0.13
			21, 13	23, 12	16	16	
			19, 13	22, 12	15	15	
			18, 13	16, 12	15	14	
			20, 12	18, 14	15	16	
1.14	398	0.131	24, 19	26, 20	21	22	0.83 ± 0.12
			28, 15	21, 21	19	21	
			23, 18	23, 18	20	20	
			23, 20	22, 19	21	21	
			25, 18	24, 21	21	22	
1.41	439	0.124	42, 25	37, 29	31	33	0.79 ± 0.12
			52, 35	39, 30	42	34	
			39, 33	37, 42	36	39	
			35, 34	37, 34	35	35	
			34, 31	43, 30	32	35	
Adhesive C							
0.52	433	0.094	10, 11	11, 11	10	11	0.33 ± 0.05
			10, 10	9, 11	10	10	
			9, 11	8, 13	10	10	
			9, 10	14, 10	10	12	
			11, 11	9, 12	11	10	
0.71	422	0.152	15, 24	18, 16	18	17	0.42 ± 0.06
			15, 22	17, 19	18	18	
			15, 22	15, 22	18	18	
			17, 18	16, 19	18	18	
			16, 19	14, 24	18	17	
0.91	440	0.158	29, 26	27, 30	27	29	0.42 ± 0.06
			25, 30	26, 29	27	27	
			31, 31	23, 32	31	26	
			30, 30	27, 39	30	28	
			26, 35	34, 26	30	30	
1.14	398	0.131	79, 82	70, 72	41	45	0.31 ± 0.08
			75, 81	67, 73	64	49	
			70, 71	78, 84	71	52	
			71, 76	81, 72	59	45	
			80, 74	75, 79	47	47	
1.41	439	0.124	41, 41	37, 58	80	71	0.34 ± 0.10
			74, 56	48, 50	78	70	
			62, 82	51, 53	70	81	
			52, 69	48, 43	73	76	
			49, 45	42, 52	77	77	

losses. Because the total area of the adhesive was kept constant at 60×10^4 m^2, the work done fracturing the adhesive was estimated by multiplying the toughness by this area. A comparison between Equations 4 and 8 shows that the work dissipated in plastically deforming both arms of the test sample in $1/n$, or approximately four times, the energy absorbed by the adhesive. The difference between the sum of these two energies, and the total energy dissipated, calculated from the accelerometer data, gives an indication of the magnitude of the other losses. The results for adhesive B bonding the aluminium are tabulated in Table III. It can be seen that, irrespective of the aluminium thickness, about 7% of the total energy consistently went towards fracturing the adhesive, and about 28% went into plastic deformation of the adherends. The balance

TABLE III Energy absorbed during fracture of 5754 aluminium samples bonded with adhesive B (Ciba-Geigy XD4600)

h (mm)	Γ (kJ m^{-2})	Total energy absorbed (J)	Energy absorbed by fracture (J)	% of energy total absorbed by fracture
1.0	1.33 ± 0.20	10.7 ± 0.4	0.80 ± 0.12	7 ± 1
1.3	1.30 ± 0.21	11.7 ± 0.4	0.78 ± 0.13	7 ± 1
1.6	1.56 ± 0.23	13.2 ± 0.4	0.94 ± 0.14	7 ± 1
2.0	1.36 ± 0.21	13.6 ± 0.4	0.82 ± 0.13	6 ± 1
2.3	1.56 ± 0.25	13.5 ± 0.4	0.94 ± 0.15	7 ± 1
3.0	1.43 ± 0.21	14.3 ± 0.4	0.86 ± 0.13	6 ± 1

of about 65% was absorbed by other losses associated with the impact and with friction. High-speed infrared photography conducted during the course of similar experiments, showed fairly high temperatures being generated by the passage of the sample over the wedge [13].

4. Discussion

The test geometry described in this paper has unique features that make both the analysis and interpretation of the experiments particularly useful. Because all the plastic deformation is directly associated with the fracture process it can be used directly as an analytical tool to analyse failure. This should be contrasted with both the peel test [6] and the constrained variant of the wedge-impact test [14, 15] where there is extensive bending and stretching in the wake of the crack away from the tip. The deformation in these two tests is incidental to crack-tip events, and therefore cannot be used to interpret the fracture process. The ability to use observations of the deformation to deduce the stresses associated with fracture means that a measurement of the applied load is not needed. This is important, because, even in this geometry, the applied load includes components that are extraneous to fracture events, such as friction. In the peel test and constrained wedge-impact tests, the applied load contributes to deformation in the wake of the crack. Therefore, any schemes that use the load to extract a measure of the toughness of a joint inevitably involve subtraction of two large numbers (the work done by the loads and energy absorbed by processes other than fracture) [5]. This can lead to large levels of uncertainty in the values obtained. In contrast, the test described in this paper, with its direct observation of the plastic deformation and use of Equation 10 to obtain the toughness, avoids this problem.

The technique has been used to compute the toughness of joints made with three commercial structural adhesives bonded to different thicknesses of adherends. Despite large differences in the deformation of the samples, remarkably consistent values for the toughness of each adhesive on a particular substrate were obtained. The variation of the toughness with thickness was well within the $\sim 15\%$ experimental error estimated for these experiments. Furthermore, these results were tested for reproducibility by having different members of the research team independently make, test and analyse the samples. Irrespective of who did the different tasks, the results for the toughness were always reproducible.

The sensitivity of the results to the choice of the power-law used to describe the adherends was investigated by numerically integrating the stress–strain data to obtain an energy-release rate (instead of using Equation 8). Using numerical integration rather than a curve-fitting approach allowed the initial linear-elastic portion of the deformation (as well as the spring-back) to be included in the analysis. The numerical analyses did not give significantly different results for the toughness. Furthermore, it was noted that while the experimental stress–strain data could be fitted by a number of slightly different values for the power-law coefficients, the resultant values of toughness were not perturbed significantly, as long as a good fit in the appropriate strain range was maintained. For example, when a different aluminium alloy was used with very different work-hardening characteristics for one set of data, the results fell into line with the other aluminium joints once the appropriate values for A and n had been measured and incorporated in the analysis.

The reproducibility of the results suggests that toughness values falling far outside the 15% range of uncertainty have to be considered significant. Two aspects of the results must therefore be noted. The first is a comparison between the toughness values obtained for the plastically deforming joints and those obtained for the same adhesives tested under elastic conditions. A double-cantilever beam specimen of sufficiently large dimensions to ensure that yielding did not occur prior to fracture was used to determine the toughness values for joints made with adhesives B and C on a high-yield stress steel. It was found that the toughness was ~ 1.2 J m^{-2} for adhesive B and ~ 1.0 J m^{-2} for adhesive C. These should be compared with the values of toughness given in Table II of 0.80 J m^{-2} and 0.36 J m^{-2} for adhesives B and C on steel, respectively. The fact that higher values of toughness were obtained under elastic conditions is consistent with the results of Kinloch *et al.* [16] who used tapered-double-cantilever-beam specimens to measure the toughness of adhesives A and B on an aluminium alloy. They reported a value of $\mathcal{G}_{Ic}$ between 3.7 kJ m^{-2} and 4.7 kJ m^{-2} (depending on the crack velocity) for a joint made with adhesive A, and a toughness of between 2.4 kJ m^{-2} and 2.8 kJ m^{-2} for a joint made with adhesive B [16]. While further work is clearly needed to understand the difference between

the results, it should be noted that the deformation of polymers is very sensitive to the stress state [17]. It is possible, perhaps, that the stress state ahead of a crack tip surrounded by an elastic field is more efficient at activating toughening mechanisms in these adhesives than the stress-state ahead of a crack in a plastically deforming joint. In any case, it should be noted that the LEFM results of Kinloch *et al.* [16] cannot be used to predict the extent of plastic deformation associated with failure in the present experiments. Use of the higher values of toughness would result in predicted deformations far in excess of what was observed, and out of the bounds of any reasonable level of uncertainty associated with interpretation of the data.

A second result noted from these experiments is that, while there was excellent consistency for the values of toughness obtained for each adhesive on a particular substrate, a significant difference was detected between the steel and aluminium samples. This was also unexpected, and a number of possible explanations have been considered. As described earlier, the effect of elastic spring-back was ignored. The radius of curvature at the instant of fracture was taken to be that measured when the loads had been removed. The actual radius of curvature would have been somewhat smaller because of spring-back, but this effect is small except for the samples with very large curvatures. However, in these cases the uncertainty associated with the curvature measurements becomes increasingly significant and is more important than spring-back effects. It was also observed that while, in general terms, the adhesive failed cohesively, the metal–adhesive interface did frequently appear to influence the fracture process. Sometimes the crack would run close to one interface; sometimes it would jump from one interface to another. The magnitude of the difference between the results obtained from the aluminium and steel samples suggests that there was a real difference in the toughness. In this context, it should be noted that a difference in adhesive toughness has been previously reported by Armstrong [18] on aluminium and carbon composite substrates. It is quite possible that there is a difference in how the epoxy adhesives cure on the aluminium and the steel substrates. This difference in toughness between the two systems is the subject of ongoing investigation.

5. Conclusions

An analysis has been presented for the crack-driving force in an adhesive joint being separated by bending moments when the adherends undergo plastic deformation. This expression can be used to obtain a value for the intrinsic toughness of the adhesive by measuring the applied moments at fracture. Furthermore, it has also been demonstrated that the toughness can be obtained very straightforwardly by measurements of the plastic deformation of the fractured samples. Indeed, this leads to the remarkable conclusion that, provided the constitutive properties of the adherends are known, the toughness of an adhesive can be obtained in a test involving no more instrumentation than a ruler!

This analysis has been used as the basis for interpreting the data from a wedge-impact test. The values for the toughness of the joint were shown to be consistent, within the experimental error of the tests, for a range of different thickness of adherends. The values were dependent only on the materials used to form the bond, and were very reproducible. However, there were unexplained differences between these values, and those obtained by LEFM techniques.

Acknowledgements

This work was supported by Ford Motor Co., a Rackham Faculty Grant from the University of Michigan, and NSF Grant No. CMS 9 624 452. The authors would like to thank W. S. Stewart, M. A. DeBolt and R. Perry of Ford Motor Co. for experimental help, and Y. Wu for proof reading the manuscript.

References

1. D. A. WAGNER, C. M. CUNNINGHAM and M. A. DEBOLT, in Proceedings of the International Body Engineering Conference, Detroit, MI, 21–23 September (1993) 123–8.
2. A. J. KINLOCH, "Adhesion and adhesives, science and technology" (Chapman and Hall, London, 1987) pp 194–9.
3. A. N. GENT and A. J. KINLOCH, *J. Poly. Sci. A*2 **9** (1971) 659.
4. A. GLEDHILL, A. J. KINLOCH, S. YAMANI, R. J. YOUNG, *Polymer* **19** (1978) 574.
5. K. S. KIM, *Mater. Res. Soc. Symp. Proc.* **119** (1988) 31.
6. J. KIM, K. S. KIM and Y. H. KIM, *J. Adhesion Sci. Technol.* **3** (1989) 175.
7. J. R. RICE, *J. Appl. Mech.* **35** (1968) 379.
8. R. A. SMITH, *Mater. Engng Appl.* **1** (1979) 316.
9. M. D. CHANG, K. L. DEVRIES and M. L. WILLIAMS, *J. Adhesion* **4** (1972) 221.
10. R. A. SCHAPERY, *Polym. Engng Sci.* **27** (1987) 63.
11. Z. SUO and J. W. HUTCHINSON, *Int. J. Fracture* **43** (1990) 1.
12. S. M. WARD, M. A. DEBOLT, G. L. WESTERBEEK and R. A. DICKIE, in Proceedings of the 18th Annual Meeting of the Adhesion Society, Hilton Head, SC, 19–22 February (1995) p. 255.
13. R. A. DICKIE and S. M. WARD, in "Mittal Festschrift", edited by W. J. van Ooij and H. R. Anderson Jr (VSP, Zeist, The Netherlands, 1997) pp. 1–13.
14. ISO 11 343, "Adhesive; determination of dynamic resistance to cleavage of high strength adhesive bonds under impact conditions: wedge impact method" (International Organization for Standards, Geneva, Switzerland 1993).
15. A. C. TAYLOR, B. R. K. BLACKMAN, A. J. KINLOCH and Y. WANG, in Proceedings of the 19th Annual Meeting of the Adhesion Society, Myrtle Beach, SC, 18–21 February (1996) p. 225.
16. A. J. KINLOCH, B. R. K. BLACKMAN, A. C. TAYLOR and Y. WANG, in Proceedings of the Euradh '96 Conference, Institute of Materials, London, 3–6 September (1996) pp. 467–71.
17. R. J. YOUNG, "Introduction to polymers" (Chapman & Hall, London, 1981) pp. 264–7.
18. K. B. ARMSTRONG, *Int. J. Adhesion Adhesives* **16** (1996) 21.

Received 23 May 1996
and accepted 7 July 1997